Influence of the environment potential on the structural and dynamical properties of ionic crystals

Claus Falter, Georg A Hoffmann and Frank Schnetgöke

Institut für Theoretische Physik II—Festkörperphysik, Universität Münster,
Wilhelm-Klemm-Strasse 10, 48149 Münster, Germany

Abstract. The effect of two different approaches to the environment potential on structural, screening and lattice dynamical properties of ionic crystals is calculated using a microscopic model recently proposed. One approach is the conventional Madelung procedure for the potential depth and the other is based on the minimization of the total energy of the crystal. Results are presented for the typical ionic crystals NaCl and MgO.

1. Introduction

In this paper we investigate the influence of a suitably chosen environment potential on the dynamical and static properties of ionic crystals. Such a potential appears as an element of our theoretical model to investigate the electronic density response, electron–phonon interaction (EPI) and the lattice dynamics in ionic materials and in particular in the high-temperature superconductors (HTSCs) [1, 2]. In our model description for the electronic density response and the EPI the local part is approximated by an *ab initio* rigid-ion model (RIM) taking into account ion softening as calculated from a tight-binding analysis of the electronic bandstructure. The method of Gordon and Kim [3] is used to calculate the pair potentials from the ionic densities.

Such a model then serves for example as a reference system for the insulating phase of the HTSC. For a description of screening in particular in the metallic phase of the HTSC in addition more or less localized electronic charge fluctuations (CFs) on the outer shells of the ions are considered. While these polarization processes dominate in the metallic phase of the HTSC [1, 2, 4] they are less pronounced in classical ionic crystals. We investigated this problem in [5] for MgO. Especially the main deficiency of the RIM in the description of the lattice dynamics of ionic crystal, i.e. the overestimation of the longitudinal optical frequencies, cannot significantly be reduced by the CFs and polarization processes of dipole type (dipole fluctuations (DFs)) are of crucial importance in this case. In order to account for this, we have recently extended our theory to include an *ab initio* description of the contribution of the dipoles to the lattice dynamics and applied it to the classical ionic crystals NaCl and MgO [6]. It should be noted here that our ultimate goal is to apply our model based on the RIM and extended by screening processes of CF and DF type to the insulating phase of the HTSC which cannot be described rigorously within density functional theory (DFT) applying the local density approximation (LDA) because the LDA predicts a metallic state for these materials. The same is true even for the metallic optimal doped phase of the HTSC along the *c*-axis,

where the charge response inside a small conelike region around this axis is insulator-like as follows from the optical experiments [7]. See also the discussion given in [8] in this context.

In order to deal with the unstable oxygen anion in the corresponding materials which is stabilized only by the crystalline environment, we have used in the past the Watson sphere potential method [9], enclosing the oxygen ion in a (Watson) sphere with opposite charge. The radius of the sphere which also determines the depth of the potential was fixed to give the Madelung potential at the site of the oxygen ion in the crystal. This somewhat arbitrary procedure which on the other hand has characteristic effects on the ion density and all the resulting quantities (lattice structure, electronic polarization processes like CFs and DFs, phonon frequencies etc) will be replaced in the present paper by a more systematic one, minimizing the total energy of the crystal as a function of the radius or equivalently the potential depth of the Watson sphere potential at the anion.

We present in section 2 a short review of some aspects of our theoretical model so that the paper is sufficiently complete in itself. In section 3 we compare, using NaCl and MgO as examples, the effects of the energy minimization procedure to determine the environment potential on various physical quantities with the corresponding effects as obtained from the Madelung potential approach. A summary and outlook is given in section 4. Finally, the form of the *ab initio* pair potential is listed in an appendix.

2. Sketch of the theoretical model

This section deals with a brief résumé of the theory and the model. More details can be found in our previous work [1, 2, 6]. The starting point of our considerations is the densities of the ions represented as

$$\rho_\alpha(\vec{r}) = \rho_\alpha^0(r) + \sum_\lambda Q_\lambda \rho_\lambda^{CF}(r) + \vec{p}_\alpha \hat{r} \rho_\alpha^D(r). \tag{1}$$

$\rho_\alpha^0(r)$ is the density of the unperturbed ion, assumed to be spherically symmetric and localized at the sublattice α of the crystal. The second contribution in equation (1) describes the charge fluctuations (CFs) in the electronic orbitals λ with amplitude Q_λ and form factor (density distribution) $\rho_\lambda^{CF}(r)$. The last term in (1) represents the dipolar deformation of an ion α with amplitude (dipole moment) $\vec{p}_\alpha$ and the radial density distribution $\rho_\alpha^D(r)$. $\hat{r}$ is the unit vector in the direction of $\vec{r}$. The $\rho_\lambda^{CF}(r)$ are approximated by a spherical average of the orbital densities of the outer ionic shells calculated in LDA and taking self-interaction effects (SIC) into account. For the dipole density $\rho_\alpha^D(r)$ we use the charge redistribution at an ion as induced by a homogeneous electric field. This redistribution is calculated with a (modified) Sternheimer method in the framework of DFT–LDA–SIC, see e.g. [6, 10].

In the next step we investigate the total energy of the crystal according to the Gordon–Kim approach [3] assuming the density of the crystal to be given by a superposition of overlapping densities of the individual ions. The latter are calculated within SIC–LDA [11]. Experimental measurements of the electron density in ionic crystals confirm such an approximation by overlapping ionic densities [12]. Introducing additionally effective ionic charges together with the Watson sphere approach, such an approximation is also applicable to the HTSCs [1, 2, 13].

In our model description the ion softening resulting in effective ionic charges is obtained from a tight-binding analysis of the electronic bandstructure by calculating the orbital occupation numbers Q_μ of the μth (tight-binding) orbital in question, i.e.

$$Q_\mu = \frac{2}{N} \sum_{n\vec{k}} |C_{\mu n}(\vec{k})|^2. \tag{2}$$

$C_{\mu n}(\vec{k})$ means the μth component of the eigenvector of band n at the wavevector $\vec{k}$ from the first Brillouin zone and the summation in equation (2) runs over all occupied states. N denotes the number of elementary cells in the (periodic) crystal. For NaCl and MgO we have obtained for the effective ionic charges $|Z| = 0.98$ and $|Z| = 1.91$, respectively, while the ion-softening effect in the HTSC is much stronger, pointing to a growing importance of covalence effects in these materials. For La_2CuO_4 we find for example $La^{2.28+}$, $Cu^{1.22+}$, $O_{xy}^{1.42-}$, $O_z^{1.47-}$ [2, 5].

The second aspect besides ion softening in the calculation of the density of the ions, namely, the improvement of the environment potential, is the main subject of our investigations in this paper.

Applying additionally the pair-potential approximation we obtain the following result for the total energy in our model:

$$E(R, \zeta) = \sum_{\vec{a}\alpha} E_{s\alpha}^{\vec{a}} + \frac{1}{2} {\sum_{\substack{\vec{a}\alpha \\ \vec{b}\beta}}}' \phi_{\alpha\beta}(\vec{R}_\beta^{\vec{b}} - \vec{R}_\alpha^{\vec{a}}). \tag{3}$$

The energy becomes a function of the configuration of the ions $\{R\}$ and the total of the electronic degrees of freedom (EDFs) $\{\zeta\}$ of the density, i.e. $\{Q_\lambda\}$ and $\{\vec{p}_\alpha\}$ in equation (1). $E_{s\alpha}^{\vec{a}}$ are the (self-) energies of the individual ions. $\vec{a}, \vec{b}$ denote the elementary cells in the crystal and α, β the sublattices ($\vec{R}_\alpha^{\vec{a}} \equiv \vec{R}^{\vec{a}} + \vec{R}^\alpha$). The second term in (3) gives the interaction energy E_{ii} of the system expressed by the sum of pair interactions $\phi_{\alpha\beta}(\vec{R})$ between a pair of ions (α, β) connected by the vector $\vec{R}$. The prime in (3) means that the self-term has to be left out in the summation. $E_{s\alpha}^{\vec{a}}$ as well as $\phi_{\alpha\beta}(\vec{R})$ in general depend upon ζ via ρ_α; however, this relationship has been suppressed in our notation. The explicit form of the pair potential has been given in [6] and is also listed in the appendix of this paper.

According to the adiabatic principle, for a given ion configuration $\{R\}$ the electronic degrees of freedom $\{\zeta\}$ adjust such that the energy is minimized, i.e.

$$\frac{\partial E(R, \zeta)}{\partial \zeta} = 0 \tag{4}$$

for any configuration $\{R\}$. Equation (4) can be used to derive an expression for the force constants and accordingly the dynamical matrix in the harmonic approximation:

$$t_{ij}^{\alpha\beta}(\vec{q}) = [t_{ij}^{\alpha\beta}(\vec{q})]_{RIM} - \frac{1}{\sqrt{M_\alpha M_\beta}} \sum_{\kappa,\kappa'} [B_i^{\kappa\alpha}(\vec{q})]^* [C^{-1}(\vec{q})_{\kappa\kappa'}][B_j^{\kappa'\beta}(\vec{q})]. \tag{5}$$

$t_{ij}^{\alpha\beta}(\vec{q})$ are the elements of the dynamical matrix at wavevector $\vec{q}$ from the first Brillouin zone, $[t_{ij}^{\alpha\beta}(\vec{q})]_{RIM}$ denotes the contribution of the rigid ion model (RIM), M_α and M_β represent the masses of the ions and the quantities $\vec{B}(\vec{q})$ and $C(\vec{q})$ describe the Fourier transforms of the coupling coefficients

$$\vec{B}_{\kappa\beta}^{\vec{a}\vec{b}} = \frac{\partial^2 E(R, \zeta)}{\partial \zeta_\kappa^{\vec{a}} \partial \vec{R}_\beta^{\vec{b}}} \tag{6}$$

and

$$C_{\kappa\kappa'}^{\vec{a}\vec{b}} = \frac{\partial^2 E(R, \zeta)}{\partial \zeta_\kappa^{\vec{a}} \partial \zeta_{\kappa'}^{\vec{b}}}. \tag{7}$$

The derivatives in (6) and (7) have to be taken at the equilibrium positions. κ describes the EDF (charge fluctuations and dipole fluctuations in our model) localized in an elementary cell of the crystal. For the details of the calculation to obtain $\vec{B}$ and C we refer to our earlier work e.g. [1, 5, 6].

In the case where we take in the calculation for the ionic density a Watson sphere potential into account in order to include approximately the influence of the crystalline environment, the total energy of the crystal additionally depends on the corresponding Watson radii R_{ws} or equivalently on the depths $V_{ws}^{(0)}$ of the Watson sphere potentials.

$$
V_{ws}(r, V_{ws}^{(0)}) = \begin{cases} V_{ws}^{(0)} & \text{for } r \leqslant R_{ws} \\ \dfrac{Z}{r} & \text{for } r > R_{ws} \end{cases} \tag{8}
$$

with

$$
R_{ws} = \frac{Z}{V_{ws}^{(0)}}. \tag{9}
$$

In the conventional approach we also have used so far, $V_{ws}^{(0)}$ is taken to be (minus) the Madelung potential at the site of the ion in the crystal. In this paper we focus on a more systematic procedure to fix R_{ws} or $V_{ws}^{(0)}$, respectively, by minimizing the total energy of the crystal with respect to the radii R_{ws}^{α} or depths $^{\alpha}V_{ws}^{(0)}$, i.e.

$$
E_{CR} = \min_{\{^{\alpha}V_{ws}^{(0)}\}} \min_{\{R\}} E(R, \zeta = 0; \{^{\alpha}V_{ws}^{(0)}\}) \tag{10}
$$

$$
E(R, \zeta = 0; \{V_{ws}^{(0)}\}) = \sum_{\vec{a}\alpha} E_{s\alpha}^{\vec{a}}(^{\alpha}V_{ws}^{(0)}) + E_{ii}(R, \{^{\alpha}V_{ws}^{(0)}\}). \tag{11}
$$

The self-energies of the individual ions $E_{s\alpha}^{\vec{a}}$ depend on the $^{\alpha}V_{ws}^{(0)}$ and have to be included in the minimization procedure. The self-energy for an ion α in an external potential like the Watson sphere potential is given by

$$
E_{s\alpha}(^{\alpha}V_{ws}^{(0)}) = E_{tot}^{\alpha}(^{\alpha}V_{ws}^{(0)}) - E_{ws}^{\alpha}(^{\alpha}V_{ws}^{(0)}). \tag{12}
$$

Here E_{tot}^{α} means the total energy of the ion in the external potential $^{\alpha}V_{ws}$ and E_{ws}^{α} the potential energy of the charge density ρ_{α} in the Watson sphere potential. In the context of the minimization according to equations (10), (11) the change of $E_{s\alpha}$ when $^{\alpha}V_{ws}^{(0)}$ is varied is of particular interest.

In section 3 we will study the effect of fixing the environmental potential by energy minimization as compared with the usual procedure via the Madelung potential on various properties of ionic crystals. Besides the influence on the structure, ionic polarizability and lattice dynamics we also have calculated results for the macroscopic dielectric constant, $\varepsilon_{\infty}(\hat{q})$ ($\hat{q} = \vec{q}/q$) and the transverse effective charges, Z_{α}^{T}. So we supply for completeness the expressions for these quantities within our theoretical description [6, 14].

$$
\varepsilon_{\infty}(\hat{q}) = \lim_{\vec{q} \to \vec{0}} (1/(1 - v(q)\chi_0(\vec{q}))) \tag{13}
$$

with

$$
v(q) = \frac{4\pi}{V_Z q^2} \tag{14}
$$

and

$$
\chi_0(\vec{q}) = \sum_{\kappa,\kappa'} \rho_{\kappa}(\vec{q})[C^{-1}(\vec{q})]_{\kappa\kappa'} \rho_{\kappa'}^{*}(\vec{q}). \tag{15}
$$

V_Z denotes the volume of the elementary cell and $\rho_{\kappa}(\vec{q})$ is the Fourier transform of $\rho_{\lambda}^{CF}(r)$ (charge fluctuations) and $\vec{r}\rho_{\alpha}^{D}(r)$ (dipole fluctuations), respectively. The tensor of effective charges, $\mathbf{Z}_{\alpha}^{T}$, can be obtained from the equation

$$
\hat{q}\mathbf{Z}_{\alpha}^{T}\hat{q} = \lim_{\vec{q} \to \vec{0}} \left(\varepsilon_{\infty}(\hat{q}) \left(Z_{\alpha} + \mathrm{i}\frac{\vec{q}}{q^2} \left(\sum_{\kappa} \rho_{\kappa}(\vec{q})\vec{X}^{\kappa\alpha}(\vec{q}) \right) \right) \right) \tag{16}
$$

where the quantity X is related to C and B from equations (6), (7) by

$$X = C^{-1}B \tag{17}$$

written in symbolic notation.

3. Numerical results and discussion

In the following we illustrate the energy minimization procedure to obtain the environment potential in the Watson sphere model taking NaCl as an example. Furthermore, we oppose the results for various physical properties of ionic crystals as obtained from the energy minimization with those as obtained from the conventional procedure via the Madelung potential.

In the case of NaCl we take into account a Watson sphere potential for the Cl anion. It should be noted that in general it is sufficient to consider environment potentials only for the anions; the cations are largely unaffected [6]. The calculation is performed with an effective ionic charge $|Z| = 0.98$ resulting from a tight-binding analysis of the electronic bandstructure according to equation (2).

Figure 1 displays our results for the variation of the self-energy E_{sCl} of the $Cl^{0.98-}$ ion as a function of the depth $V_{ws}^{(0)}$ of the Watson sphere potential according to equation (12). The energy has been shifted by the total energy of the $Cl^{0.98-}$ ion (-922.092 Ryd) as calculated in the absence of the Watson sphere potential. For smaller values of $|V_{ws}^{(0)}|$ both E_{tot}^{Cl} and E_{ws}^{Cl} in equation (12) decrease linearly at the same rate with increasing potential depth. For larger $|V_{ws}^{(0)}|$, E_{tot}^{Cl} deviates from linearity while E_{ws}^{Cl} continues to be linear resulting in an increase of the self-energy as shown in the figure.
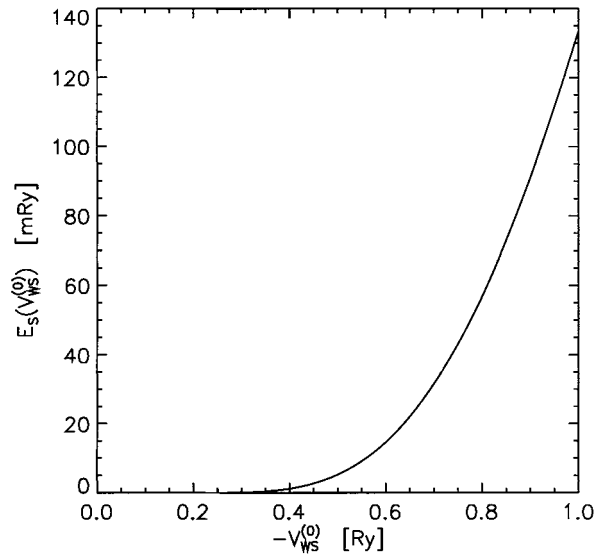
Figure 1. Self-energy E_{sCl} in mRyd of the $Cl^{0.98-}$ ion according to equation (12) as a function of the depth of the Watson sphere potential $V_{ws}^{(0)}$. The energy E_{sCl} is shifted by -922.092 Ryd which is the total energy of the $Cl^{0.98-}$ ion in the absence of a Watson sphere potential.

The curve in figure 2 represents our calculated results for the interaction energy E_{ii} of the NaCl crystal in dependence on $(-V_{ws}^{(0)})$. Adding the results for the self-energy and
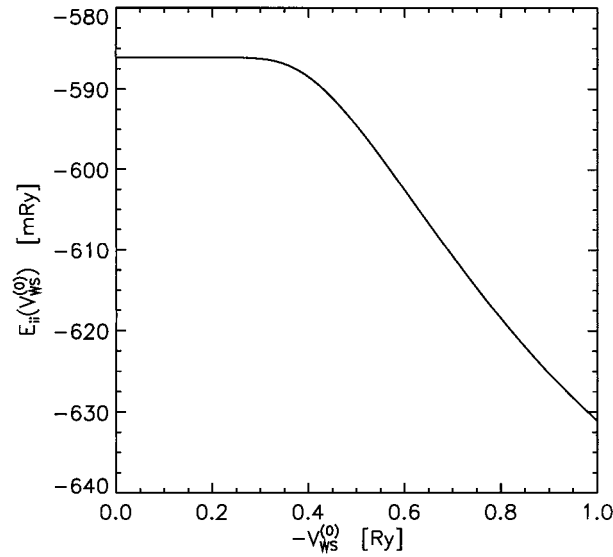
Figure 2. Interaction energy E_{ii} in mRyd of the NaCl crystal in dependence on the depth $V_{ws}^{(0)}$ of the Watson sphere potential at the $Cl^{0.98-}$ ion.

Table 1. Lattice constant, a, and depth, $V_{ws}^{(0)}$, of the environment potential of NaCl and MgO for the Madelung choice of the potential (Mad) and the result as obtained from the minimization of the total energy of the crystal (Min). Expt denotes the experimental values. a is in units of Å and $V_{ws}^{(0)}$ in units of Ryd.

|	NaCl		$-V_{ws}^{(0)}$	MgO		$-V_{ws}^{(0)}$
	a			a		
Expt	5.593	—	—	4.211	—	—
Mad	5.417	(−3.2%)	0.6482	4.114	(−2.3%)	1.6778
Min	5.492	(−1.8%)	0.5282	4.111	(−2.4%)	1.6844

interaction energy according to equation (11) we obtain the total energy of the NaCl crystal (shifted by -922.092 Ryd) as a function of $(-V_{ws}^{(0)})$. We find a minimum of the energy at $V_{ws}^{(0)} = -0.5282$ Ryd (see figure 3), which should be compared with the corresponding value $V_{ws}^{(0)} = -0.6482$ Ryd resulting from the Madelung potential using the experimental lattice constant. From these calculations we extract for NaCl a marked difference between the environment potential as obtained from the energy minimization and the conventional Madelung procedure and the question arises of what is the influence of this difference on the physical properties of ionic crystals.

In figure 4 we have calculated the effect on the structure of NaCl by investigating the dependence of the lattice constant, a, as a function of $(-V_{ws}^{(0)})$. We find an improvement for a, with regard to the experiment, when the environment potential from the energy minimization is used, see also table 1.

The influence on the polarization properties of the ions can be seen by performing calculations for the dipole polarizability α and the dipole density $\sigma^D(r)$ $(\sigma^D(r) = 4\pi r^2 \rho^D(r))$ which are both important input quantities for the lattice dynamics and the macroscopic dielectric properties of ionic crystals [6].
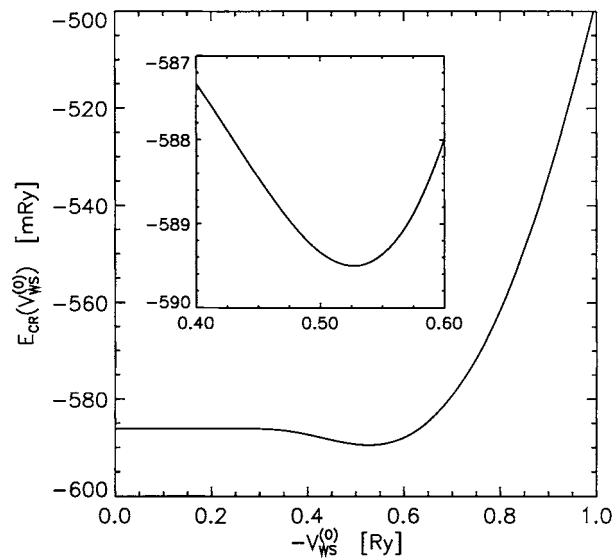
Figure 3. Total energy of the crystal according to equations (10), (11) as a function of the potential depth $V_{ws}^{(0)}$ at the $Cl^{0.98-}$ ion. The energy has been shifted by -922.092 Ryd.
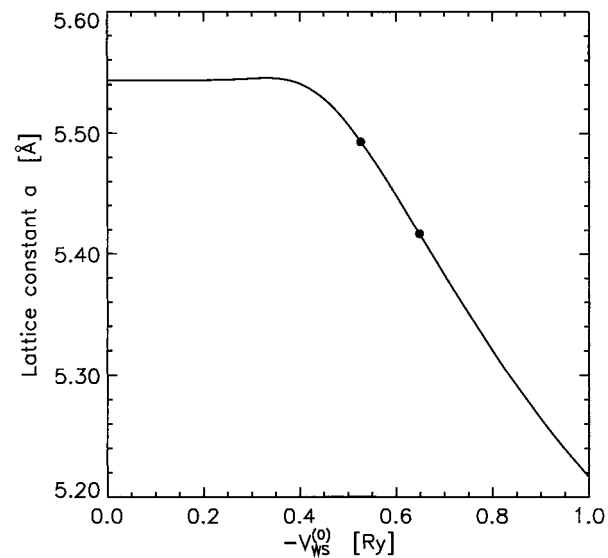

Figure 4. Lattice constant a of the NaCl crystal in units of Å as a function of $-V_{ws}^{(0)}$.

Figure 5 displays the dependence of the polarizability α for the $Cl^{0.98-}$ ion on $(-V_{ws}^{(0)})$ and from table 2 the corresponding values for α using the minimization or the Madelung procedure, respectively, can be extracted. We find an increase for the polarizability and also for the macroscopic dielectric constant ε_∞ when the minimization is used for the environment potential.

From the results for α we learn that a stronger environment potential leading in general to an increase of the binding of the electrons at the anions and consequently to a smaller
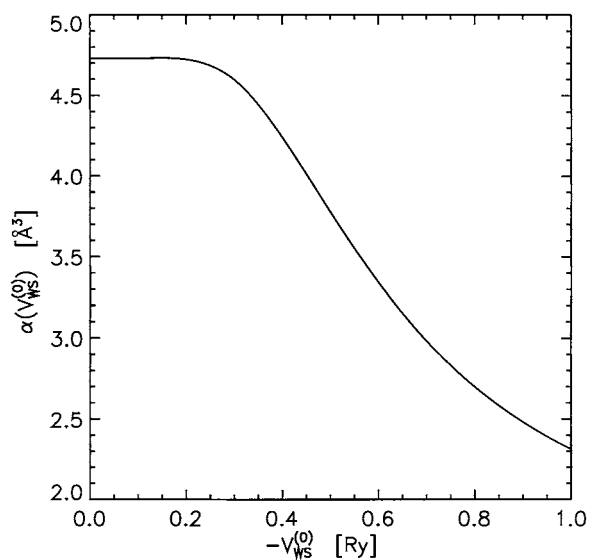
Figure 5. Dipole polarizability α of the $Cl^{0.98-}$ ion in units of $\mathring{A}^3$ as a function of $-V_{ws}^{(0)}$.

Table 2. The table collects the dipole polarizability α of the anion of NaCl and MgO in units of $\mathring{A}^3$, the macroscopic dielectric constant ε_∞ and the transverse effective charge Z^T. Ion softening is taken into account via effective ionic charges (± 0.98 for NaCl, ± 1.91 for MgO). Mad, Min, Expt have the same meaning as in table 1.

	α	ε_∞	Z^T
NaCl			
Mad	3.16	2.490	1.040
Min	3.65	2.620	1.026
Expt		2.35	1.10
MgO			
Mad	2.09	3.292	1.923
Min	2.07	3.284	1.923
Expt		2.96	1.98

polarizability α of the latter is also reflected in a contraction of the dipole density $\sigma^D(r)$ of the anions as can be read off from figure 6. Here we have shown $\sigma^D(r)$ of $Cl^{0.98-}$ for the Madelung choice of the potential (full curves) and on the other hand for the energy minimized case (dotted curves). The contraction in case of the more attractive environment potential provided by the Madelung choice can be seen clearly. The broken line in the figure displays additionally the 3p-orbital density $\rho_{3p}^0(r)$ (multiplied by $4\pi r^2$) of the unperturbed $Cl^{0.98-}$ ion for comparison. $V_{ws}^{(0)} = -0.6482$ Ryd has been used to calculate $\rho_{3p}^0(r)$.

As far as the situation for MgO is concerned, we also take ion softening in the form of effective ionic charges into account. This gives an effective charge $|Z| = 1.91$, see [5]. The energy minimization method and the Madelung procedure lead in this case (accidentally) to values of the potential depth which are virtually the same (energy minimized potential: $V_{ws}^{(0)} = -1.6844$ Ryd, Madelung choice of the potential: $V_{ws}^{(0)} = -1.6778$ Ryd). Consequently, there are practically no differences for MgO in the calculated structural and polarization properties. The definite results are contained in the tables 1 and 2. Moreover, the results
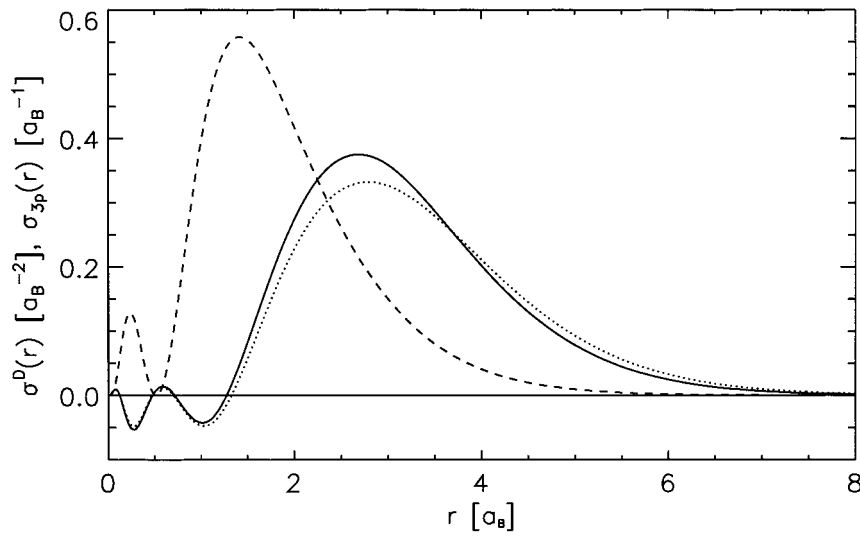
Figure 6. The full curve (——) represents the dipole density $\sigma^D(r)$ of the Cl$^{0.98-}$ ion for the Madelung choice of the environment potential ($V_{ws}^{(0)} = -0.6482$ Ryd). The dotted curve (…) illustrates the result for $\sigma^D(r)$ when the energy minimized value ($V_{ws}^{(0)} = -0.5282$ Ryd) is used. The broken line (- - -) displays the 3p orbital density $\rho_{3p}^0(r)$ (multiplied by $4\pi r^2$) of the unperturbed Cl$^{0.98-}$ ion for comparison.

for the phonon dispersion curves as calculated with our microscopic model introduced in section 2 are nearly indistinguishable in this case. Because these curves already have been published in [6] for the Madelung choice of the potential the results are not repeated in this work.

As we have seen the situation is quite different for NaCl where a marked difference in the potential depth occurs. Figure 7 contains the calculated results of the phonon dispersion curves for NaCl in the main symmetry directions $\Delta \sim (1, 0, 0)$, $\Sigma \sim (1, 1, 0)$ and $\Lambda \sim (1, 1, 1)$ for the Madelung choice of the potential and figure 8 analogous curves using for the depth of the potential the energy-minimized result. The dotted curves represent the calculated data for the RIM, the broken curves for the RIM taking additionally charge fluctuations as screening process into account. Finally, the full curves give the results for the RIM with charge fluctuation and dipole fluctuations both considered as allowed polarization processes. From an inspection of the two figures we extract that a better quality for the phonon dispersion is achieved applying the energy-minimized form of the environment potential; in particular the longitudinal optical phonons are improved considerably.

4. Summary

In this paper we have investigated the effect of two different approaches to the environment potential on structural, screening and lattice dynamical properties of ionic crystals. One approach is the conventional Madelung procedure for the potential depth and the other is a more systematic one where the depth is calculated from the minimization of the energy of the crystal within our theoretical model. We have considered so far NaCl and MgO as prototypes of typical classical ionic crystals; however, our ultimate goal is the high temperature superconductors where our theoretical model to describe the density response, electron–phonon
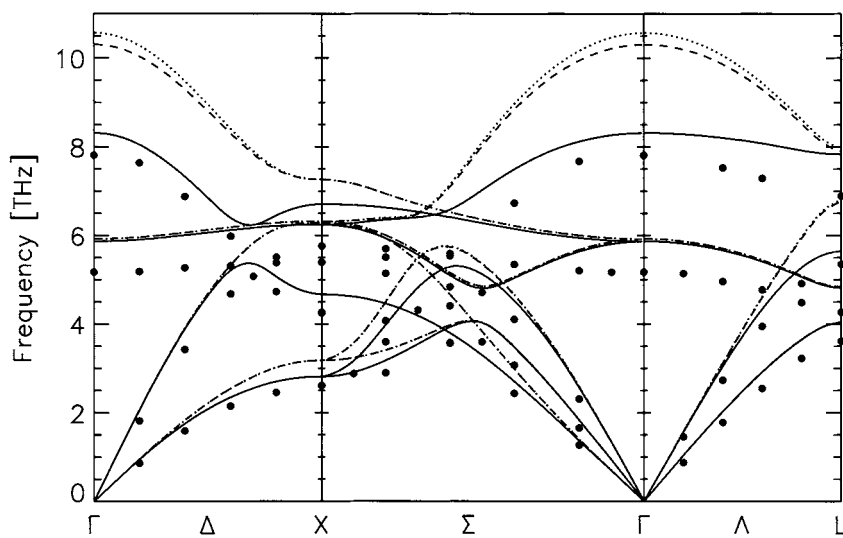
Figure 7. Calculated phonon dispersion curves for NaCl in the main symmetry directions $\Delta \sim (1, 0, 0)$, $\Sigma \sim (1, 1, 0)$ and $\Lambda \sim (1, 1, 1)$ using effective ionic charges (± 0.98) as calculated from a tight-binding analysis of the electronic bandstructure. For the $Cl^{0.98-}$ ion a Watson sphere potential in the form of the Madelung potential ($V_{ws}^{(0)} = -0.6482$ Ryd) has been applied. ($\ldots$) denotes the result for the rigid ion model (RIM), (- - - -) for the RIM + charge fluctuations (CF) and (——) for the RIM + charge fluctuations + dipole fluctuations (DF). The dots in the figure indicate the experimental data points.
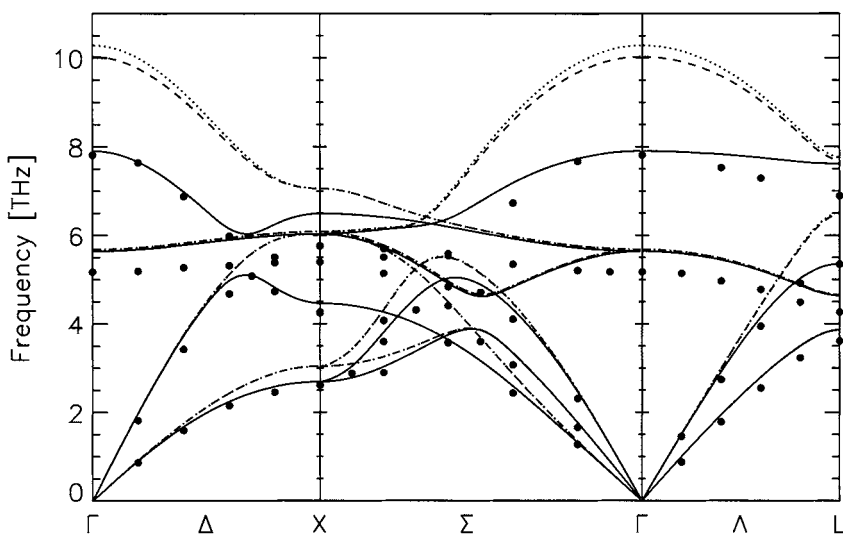
Figure 8. The same as in figure 7; however, the energy-minimized result $V_{ws}^{(0)} = -0.5282$ Ryd for the environment potential has been used.

interaction and lattice dynamics is a realistic alternative, in particular for the insulating phase where DFT–LDA calculations predict a metallic state. In the case of MgO both approaches accidentally give nearly the same value for the potential depth and consequently there are no significant differences in the calculated physical quantities. This is quite different for NaCl

where marked differences for the depth of the environment potential occur. The structural and lattice dynamical properties calculated for NaCl in the present work are better described with the energy-minimized form of the potential, while the macroscopic dielectric constant is slightly overestimated.

Acknowledgment

Appendix

In the following we present the explicit form of the pair potentials $\phi_{\alpha\beta}(\vec{R})$ in equation (3), as given in [6]. The latter can be separated into long-range Coulomb contributions and short-range terms as follows,

$$\phi_{\alpha\beta}(\vec{R}) = \frac{Z_\alpha Z_\beta}{R} - (Z_\alpha \vec{p}_\beta + Z_\beta \vec{p}_\alpha) \frac{\vec{R}}{R^3} + \vec{p}_\alpha \frac{\mathbf{1} - 3\hat{R} \otimes \hat{R}}{R^3} \vec{p}_\beta + K_\alpha U_\beta(\vec{R}) + K_\beta U_\alpha(\vec{R})$$
$$+ W_{\alpha\beta}(\vec{R}) + G_{\alpha\beta}(\vec{R}). \tag{A.1}$$

The first three terms are long-range ion–ion, dipole–ion, and dipole–dipole interactions. Z_α and Z_β are the charges of the ions. $\otimes$ denotes the dyadic product and $\hat{R} = \vec{R}/R$. The remaining terms in equation (A1) are short range. K_α and K_β are the charges of the ion cores and

$$U_\alpha(\vec{R}) = -\int dV \rho_\alpha(\vec{r}) \left[\frac{1}{|\vec{R} - \vec{r}|} - \frac{1}{R} - \frac{(\vec{r}\vec{R})}{R^3} \right] \tag{A.2}$$

$$W_{\alpha\beta}(\vec{R}) = \int dV \int dV' \rho_\alpha(\vec{r})\rho_\beta(\vec{r}') \left[\frac{1}{|\vec{r} - \vec{r}' - \vec{R}|} - \frac{1}{R} - \frac{(\vec{r} - \vec{r}')\vec{R}}{R^3} \right] \tag{A.3}$$

$$G_{\alpha\beta}(\vec{R}) = \int dV [\rho(\vec{r})\varepsilon(\rho(\vec{r})) - \rho_\alpha(\vec{r})\varepsilon(\rho_\alpha(\vec{r})) - \rho_\beta(\vec{r} - \vec{R})\varepsilon(\rho_\beta(\vec{r} - \vec{R}))] \tag{A.4}$$

Table A1. Fit parameters α, β and γ for the short-range part of the *ab initio* rigid-ion pair potentials of NaCl and MgO. β is in units of $1/a_B$ and γ in a_B. The separate contributions $K_\beta U_\alpha(R)$, $K_\alpha U_\beta(R)$, $G_{\alpha\beta}^{kin}(R)$, $W_{\alpha\beta}(R)$, $G_{\alpha\beta}^{xc}(R)$ are listed from top to bottom for each ion pair in the table. For the contributions $W_{\alpha\beta}(R)$ and $G_{\alpha\beta}^{xc}(R)$ the minus sign in equation (A.6) is valid.

	α	β	γ		α	β	γ
Na–Na	1.275	−1.855	−3.552	Mg–Mg	0.347	−1.712	2.741
	1.275	−1.855	−3.552		0.347	−1.712	2.741
	−0.057	−1.565	1.456		0.847	−1.555	0.720
	1.992	−1.829	−3.462		1.228	−1.711	2.064
	−6.076	−0.902	14.066		−3.435	−0.951	5.223
Na–Cl	0.648	−1.764	−0.426	Mg–O	1.139	−1.833	−0.250
	4.519	−1.820	0.810		4.069	−1.954	1.211
	4.575	−1.680	−0.399		3.245	−1.667	1.597
	4.643	−1.792	0.788		3.821	−1.859	1.570
	1.843	−1.331	0.504		0.199	−1.222	2.614
Cl–Cl	4.963	−1.821	0.791	O–O	3.685	−1.956	1.152
	4.963	−1.821	0.791		3.685	−1.956	1.152
	5.598	−1.423	−2.948		4.982	−1.542	−2.013
	6.268	−1.685	−1.253		5.272	−1.807	−0.549
	3.056	−1.099	−2.155		2.510	−1.992	−1.371

$$\rho(\vec{r}) = \rho_\alpha(\vec{r}) + \rho_\beta(\vec{r} - \vec{R}). \tag{A.5}$$

$K_\alpha U_\beta(\vec{R})$ yields the short-range contributions of the interaction between the core α and the density ρ_β according to equation (1). $W_{\alpha\beta}(\vec{R})$ represents the short-range Coulomb contribution of the interaction of the density ρ_α with the density ρ_β, and $G_{\alpha\beta}(\vec{R})$ is the sum of the kinetic one-particle and the exchange–correlation (XC) contribution of the interaction between the two ions.

From the $\phi_{\alpha\beta}(\vec{R})$ the coupling coefficients defined in equations (6), (7) and the pair potentials needed for the RIM can be calculated as discussed in [6]. The short-range part of the rigid-ion pair potentials and the various coupling coefficients are calculated numerically for a set of distances R between the ions. This is done for each contribution in equation (A1) separately. The corresponding result is then described for convenience by an analytic function of the form

$$f(r) = \pm \exp(\alpha + \beta R + \gamma/R) \tag{A.6}$$

where α, β, γ are fit parameters. As an example the results for these parameters are given in the case of the rigid-ion pair potentials for NaCl and MgO in table A1. The results for the coupling coefficients $\vec{B}_{\kappa\beta}^{\vec{a}\vec{b}}$ and $C_{\kappa\kappa'}^{\vec{a}\vec{b}}$ are too numerous to be given here.

References

[1]   Falter C, Klenner M and Ludwig W 1993 *Phys. Rev.* B **47** 5390
[2]   Falter C, Klenner M and Hoffmann G A 1995 *Phys. Rev.* B **52** 3702
[3]   Gordon R G and Kim Y S 1972 *J. Chem. Phys.* **56** 3122
[4]   Falter C, Klenner M, Hoffmann G A and Chen Q 1997 *Phys. Rev.* B **55** 3308
[5]   Falter C, Hoffmann G A and Klenner M 1996 *Phys. Rev.* B **53** 14 917
[6]   Falter C, Klenner M, Hoffmann G A and Schnetgöke F 1999 *Phys. Rev.* B **60** 12 051
[7]   Henn R, Kircher J and Cardona M 1996 *Physica* C **269** 99
[8]   Falter C, Klenner M and Hoffmann G A 1998 *Phys. Rev.* B **57** 14 444
[9]   Watson R E 1958 *Phys. Rev.* **111** 1108
[10] Mahan G D and Subbaswamy K R 1990 *Local Density Theory of Polarizability* (New York: Plenum)
[11] Perdew J P and Zunger A 1981 *Phys. Rev.* B **23** 5048
[12] Ivanov O V and Maksimov E G 1995 *Zh. Eksp. Teor. Fiz.* **81** 1008
[13] Krakauer H, Pickett W E and Cohen R E 1988 *J. Supercond.* **1** 111
[14] Klenner M, Falter C and Chen Q 1994 *Ann. Phys. Lpz.* **3** 225